International Journal of Engineering Research and Development

DOI: 10.29137/ijerad.1439924

Volume:17 Issue:1 Pages:44-54 March/2025

Research Article

Design and Performance Analysis of Multiband Microstrip Antenna for Wireless Communication Applications

Hakan Kisioglu [1]

[1]*Faculty of Engineering and Architecture, Department of Electrical and Electronics Engineering, Yozgat Bozok University, Yozgat, Turkey*

Received:*19/02/2024* ***Accepted:*** *28/06/2024* ***Published Online:*** *15/03/2025*
Final Version*: 01/03/2025*

Abstract

This study presents a multiband microstrip antenna designed and analyzed for wireless communication applications. The proposed antenna (Prop-Ant) is designed on a FR-4 substrate material. The Prop-Ant has dimensions of 37.5 × 46 × 1.6 mm^3. 3D electromagnetic simulation software was used to design and analyze the antenna. The simulation results indicate that the antenna, with the specified dimensions, achieves a reflection coefficient of less than 10dB in the targeted frequency ranges. In the simulation, the Prop-Ant operates at resonant frequencies of 2.45GHz, 4.78GHz and 7.6GHz with bandwidths of approximately 46.12 % (2.09 GHz - 3.22 GHz), 45.18 % (3.75 GHz - 5.91 GHz) and 25.92 % (6.51 GHz - 8.48 GHz), respectively. The simulation results show that the Prop-Ant has peak gains of 2.27dBi, 3.63dBi and 4.28dBi at resonant frequencies of 2.45GHz, 4.78GHz and 7.6GHz, respectively. The Prop-Ant exhibits high gain, good efficiency and multiband performance, indicating that it can be used in wireless communication systems.

Key Words

"Antenna, Microstrip, Multiband"

Corresponding Author: *hakan.kisioglu@bozok.edu.tr*

1. Introduction

The rapid development of wireless communication technology in recent years has led to an improved demand for multiband wireless mobile terminals. Hence, it is important to design multiband antennas that are compact, low-profile and low-cost. Several antenna types have been proposed to perform these functions (Goswami et al., 2018; Ran et al., 2020; Verma & Kumar, 2014). Wireless communication technologies such as radio frequency identification (RFID), worldwide interoperability for microwave access (WiMAX) and wireless local area network (WLAN) are widely used. RFID operations are typically allocated to the 0.92/2.45/5.8 GHz bands. WiMAX operates in the 2.5/3.5/5.5 GHz bands and WLAN operates in the 2.4/5.2/5.8 GHz bands (Li et al., 2014). Furthermore, according to (Radar Systems Panel, 2019), C-band covers frequencies between 4GHz - 8GHz, while X-band covers frequencies between 8GHz - 12GHz.

Using a separate antenna for each application increase the size and space requirements of the system (Mahendran et al., 2021). Therefore, modern wireless communication requires a single device that can support multiple technologies. Multiband antennas are used to meet this requirement (Sura et al., 2022). The techniques used to achieve multiband designs are diverse (Wang et al., 2021). These include loading different types of slots (Baytore et al., 2019; Bekasiewicz & Koziel, 2018), adding multiple resonant arms (Chen et al., 2017; Karthikeyan et al., 2020), applying novel feeding techniques (Abdalla et al., 2017; Kumar Sahu et al., 2017), and using metamaterial structures (Ali et al., 2018; Gao et al., 2017).

In many wireless applications, the multiband microstrip patch antenna is a preferred choice due to its light weight, cost, low profile, and multiband advantages (Benkhadda et al., 2020; He et al., 2015). They also replace the use of multiple antennas for different resonant frequencies (Bakariya et al., 2015). In microstrip patch antennas, multiband capability can be achieved by using different slot, stub, and feed techniques (Kumar Naik & Amala Vijaya Sri, 2018). This approach leads to a reduction in antenna size and improved performance in the desired frequency bands (Sri & Ketavath, 2023). In recent years, many researchers in the literature worked on dual-band (Joshi & Gond, 2019; Singh et al., 2019) and multiband (Ali et al., 2018; Brar et al., 2018; Mahendran et al., 2021; Mark et al., 2018; Sura et al., 2022; Wang et al., 2021; Yalduz & Çizmeci, 2023) antennas operating in different communication bands (WLAN, WiMAX, etc.) for wireless communication applications.

In this study, a multiband microstrip antenna for wireless communication applications is designed and analyzed. Commercial three-dimensional electromagnetic (EM) simulation software (CST) is used to design and analyze the antenna. Simulation results such as reflection coefficients, radiation patterns, and antenna gain in the specified operating frequency bands are compared. This paper consists of four sections. Section 2 contains the antenna design and geometrical structure. In Section 3, simulation results and discussions are included. Section 4 presents the conclusions of the study.

2. Antenna Design

This chapter presents the structural characteristics and design of a proposed multiband microstrip antenna for wireless communication applications. The antenna is designed on a 1.6mm-thin FR-4 substrate with copper on both sides. This substrate material has a loss tangent of 0.025 and a relative permittivity (εr) of 4.3. A 3.05 mm wide 50Ω microstrip line is used in the antenna design for good impedance matching in the desired operating bands. Figure 1 shows the geometrical configuration of the proposed antenna (Prop-Ant). Figure 1 (a) demonstrates the top side of the Prop-Ant structure and Figure 1 (b) displays the bottom side of the Prop-Ant structure. The parameters used in the design of the Prop-Ant are obtained by simulation with a computer with i7 processor and 16 GB RAM and these parameters are given in Table 1.

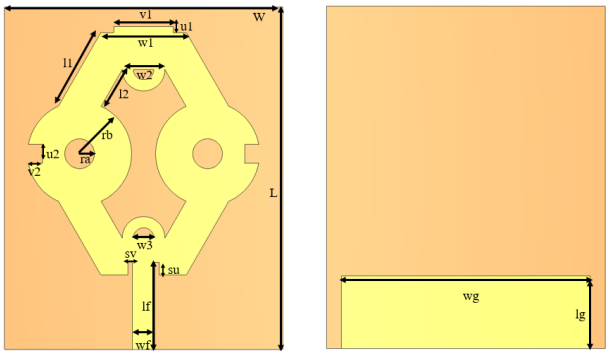

(a) **(b)**

Figure 1. Configuration of the Prop-Ant structure
The top side of the Prop-Ant structure is depicted in **(a)**, while the bottom side is illustrated in **(b)**.

Table 1. The structural parameters of the Prop-Ant

Parameters	*W*	*L*	*v1*	*u1*	*w1*	*w2*	*w3*	*l1*	*l2*	*lg*
Values (mm)	37.5	46	8	0.75	11.5	5.75	2.75	11.43	5.71	9.75
Parameters	*v2*	*u2*	*ra*	*rb*	*sv*	*su*	*lf*	*wf*	*wg*	
Values (mm)	1.89	2.5	2	7	0.6	1.7	11.7	3.05	33.5	

2.1. Antenna Design Steps

The antenna design process for multiband operation for wireless communication applications is shown in Figure 2(a). As demonstrated in the figure, the first antenna step composed of a patch structure and a ground plane. Then, the second step is obtained by hollowing out the inside of the antenna patch structure. In the third step, circles were added to the left and right sides of the antenna patch structure as shown in the figure, and circular cavities were cut in the fourth step. Squared cavities were added to the right and left sides of the circles as shown in the fifth step. In the last step, the structures shown in the figure are added to the top and bottom of the antenna patch, and the Prop-Ant patch is obtained. The resonant frequencies (2.45GHz, 4.78GHz and 7.6GHz) were obtained by modifying the ground plane of the Prop-Ant. The simulation of the reflection coefficients of the Prop-Ant design steps versus frequency is compared and presented in Figure 2 (b).

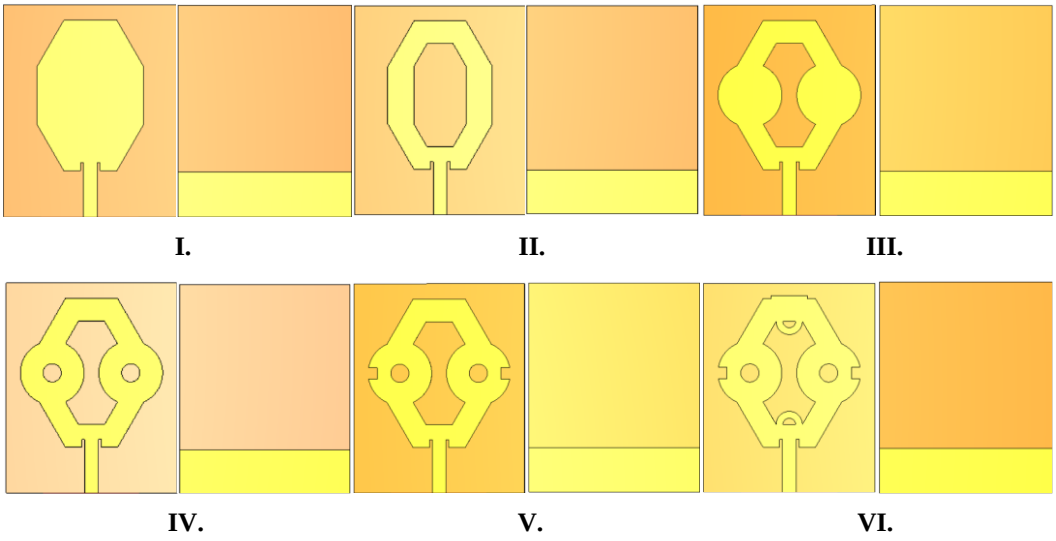

(a)

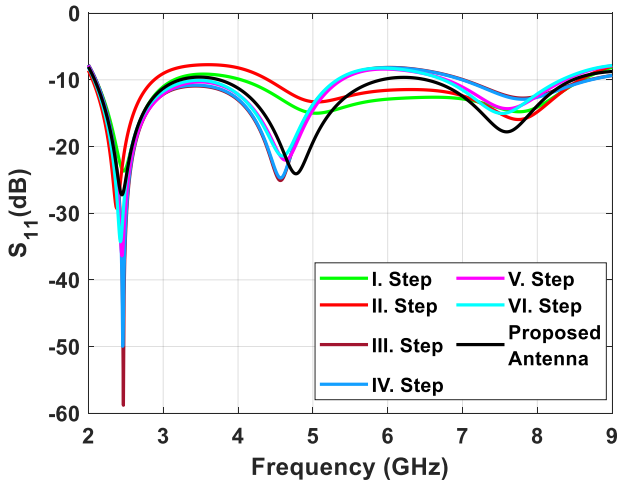

(b)

Figure 2. Design steps of the Prop-Ant **(a)** and simulation of reflection coefficients versus frequency **(b)**

3. Simulation Results and Discussions

This section presents the simulation and analysis of the antenna's reflection coefficient (S11), radiation pattern, surface current distributions, gain and radiation efficiency performance parameters. Figure 3 shows the reflection coefficient curve determined through simulation. The calculated S11 value illustrates that the antenna has three resonances at 2.45GHz, 4.78GHz and 7.6GHz according to the criterion of S11 ≤ - 10 dB. As can be obviously seen from Figure 3, the reflection coefficients (S11) at the resonant frequencies (2.45GHz, 4.78GHz and 7.6GHz) are -27.2 dB, -24.09 dB and -17.87 dB, respectively. The Prop-Ant operates in the frequency bandwidths of 46.12% (2.09-3.22) GHz, 45.18% (3.75-5.91) GHz and 25.92% (6.51-8.48) GHz, covering the RFID (2.45/5.8GHz), WiMAX (2.5/5.5GHz) and WLAN (2.4/5.2/5.8GHz) bands. The third resonant frequency operates in C-band at 7.6 GHz.

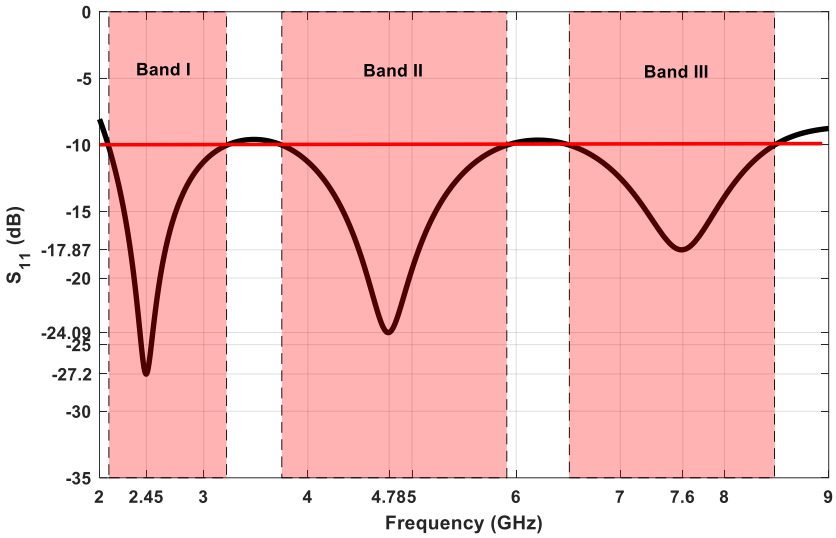

Figure 3. Simulation of reflection coefficient versus frequency

The surface current distributions of the antenna are simulated at three different resonant frequencies (2.45GHz, 4.78GHz and 7.6GHz) to investigate and verify the operating principles of the antenna design. The simulation of the surface current distributions of the Prop-Ant for three different operating frequencies is shown in Figure 4. The results show that the current distributions change for three different operating frequencies. It is observed that the surface currents are concentrated along the boundaries of the antenna geometry and at the junctions with the feed line. These results clearly show that the surface current distribution of the antenna meets the design objectives and performs well at the targeted frequencies. Figure 5 shows the simulated far-field directivity patterns of the antenna in polar coordinates at the resonant frequencies of 2.45GHz, 4.78GHz and 7.6GHz. In these figures, solid lines correspond to phi = 0 degrees and dashed lines correspond to phi = 90 degrees.

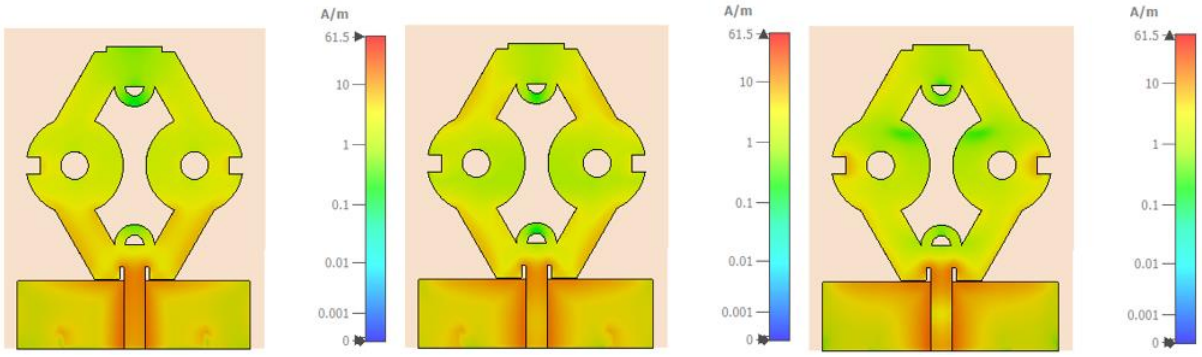

f=2.45GHz **f=4.78GHz** **f=7.6GHz**

Figure 4. Simulation of the Prop-Ant's surface current distributions for resonant frequencies of 2.45GHz, 4.78GHz and 7.6GHz

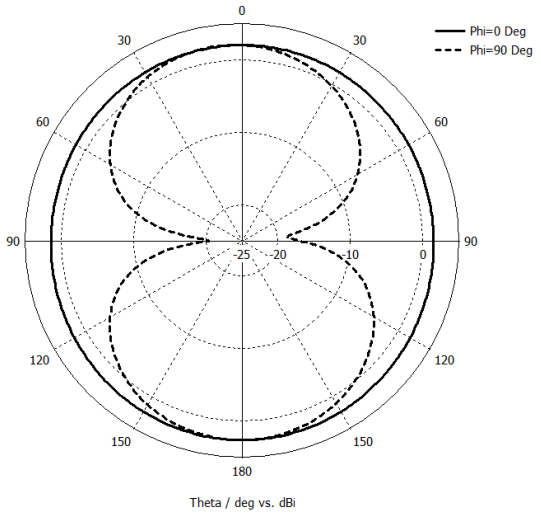

f=2.45GHz

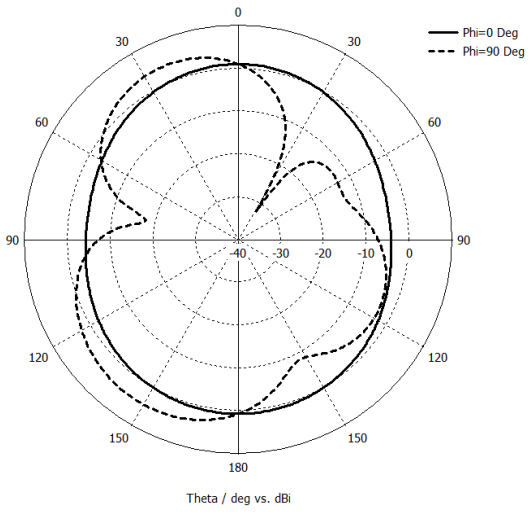

f=4.78GHz

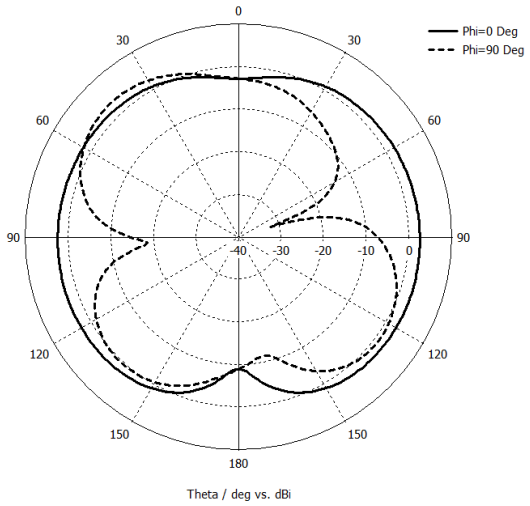

f=7.6GHz

Figure 5. Simulation of the Prop-Ant's far-field radiation patterns

There are several key parameters that influence antenna performance. Accordingly, the effects of the basic parameters are simulated and shown in Figure 6. These basic parameters are *ra*, *w2*, *u2*, *u2*, *v2*, *v2*, *v1*, *u1*, *su* and *sv* and the simulated reflection coefficients (S11) varying with these parameters are shown in Figure 6 (a)-(h). From Figures 6 (a), (d) and (f), it can be seen that the changes in the parameters *ra*, *v2* and *u1* have almost no effect on the resonant frequencies of 2.45GHz and 4.78GHz and only affect the frequency of 7.6 GHz. Figures 6 (b) and (e) show the changes in the simulated reflection coefficients with the variation in the parameters *w2* and *v1*. It can be seen that the parameters *w2* and *v1* have little effect on the frequencies of 2.45GHz and 4.78GHz compared to the frequency of 7.6 GHz. Figure 6 (c) and (h) show the variations of the simulated reflection coefficients with varying *u2* and *sv* parameters. It can be seen from these figures that the variation of *u2* and *sv* parameters has almost no effect on the resonant frequency of 2.45GHz, while it has an effect on the resonant frequencies of 4.78GHz and 7.6GHz. Figure 6 (g) shows the change in the simulated reflection coefficients with the variation in the parameter *su*. It can be seen that the variation in the parameter *su* has an effect on all three resonant frequencies. These results presented in Figures 6(a)-(h) show that the three resonant frequencies and the impedance bandwidth can be effectively controlled by adjusting the dimensions *ra*, *w2*, *u2*, *v2*, *v2*, *v1*, *u1*, *su* and *sv*.

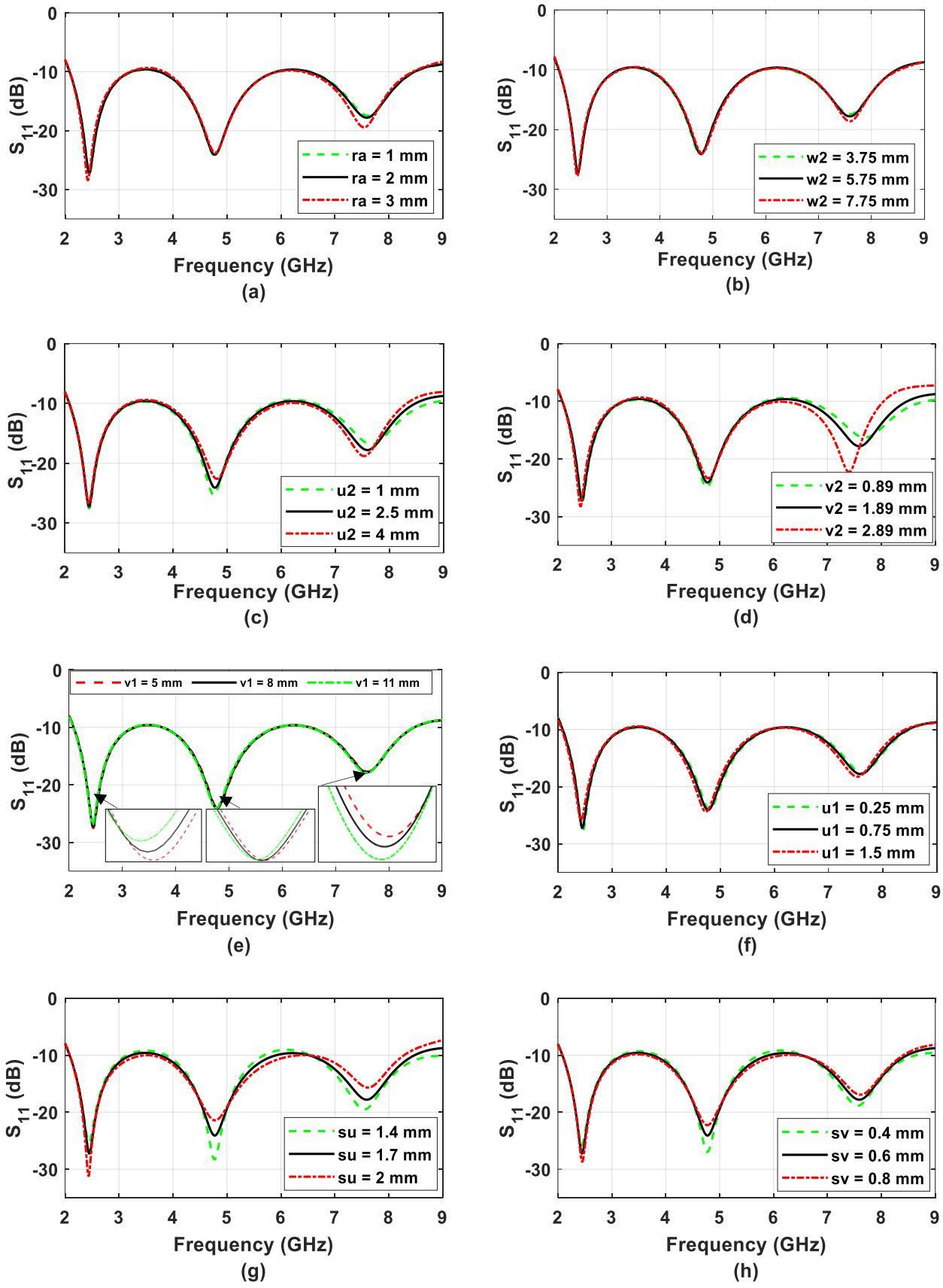

Figure 6. Simulated reflection coefficients of the Prop-Ant for parameters **(a)** *ra*, **(b)** *w2*, **(c)** *u2*, **(d)** *v2*, **(e)** *v1*, **(f)** *u1*, **(g)** *su*, **(h)** *sv*

The change of the simulated peak gain with frequency for the Prop-Ant is demonstrated in Figure 7. As can be seen from this figure, the maximum simulated peak gain of the antenna is 4.76dBi at 8GHz. Figure 8 illustrates the gain diagrams of the Prop-Ant at the resonant frequencies obtained by simulation. As can be seen from Figures 7 and 8, the peak gains at the resonant operating frequencies of 2.45GHz, 4.78GHz, and 7.6GHz are approximately 2.27 dBi, 3.63dBi, and 4.28dBi, respectively. Figure 9 shows the radiation efficiency simulation results of the Prop-Ant. At 2.45GHz, 4.78GHz, and 7.6GHz resonant frequencies, the radiation efficiencies are approximately 94.4%, 84.1%, and 76.3%, respectively. These values show that the Prop-Ant is very effective in terms of peak gain and radiation efficiency.

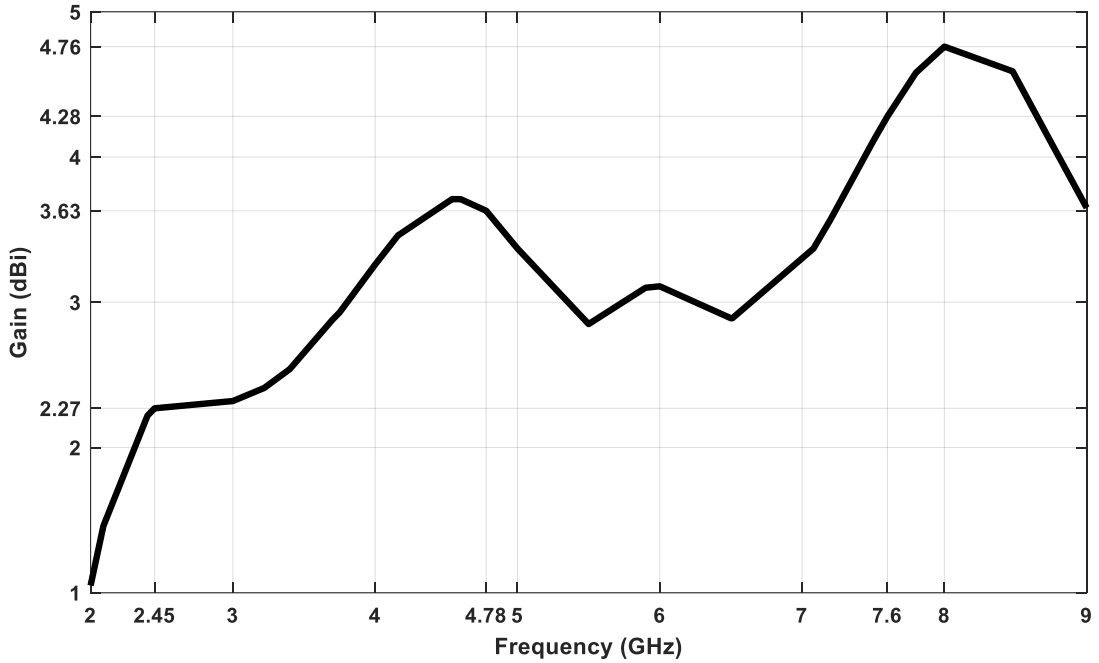

Figure 7. Simulation of the Prop-Ant's peak gain

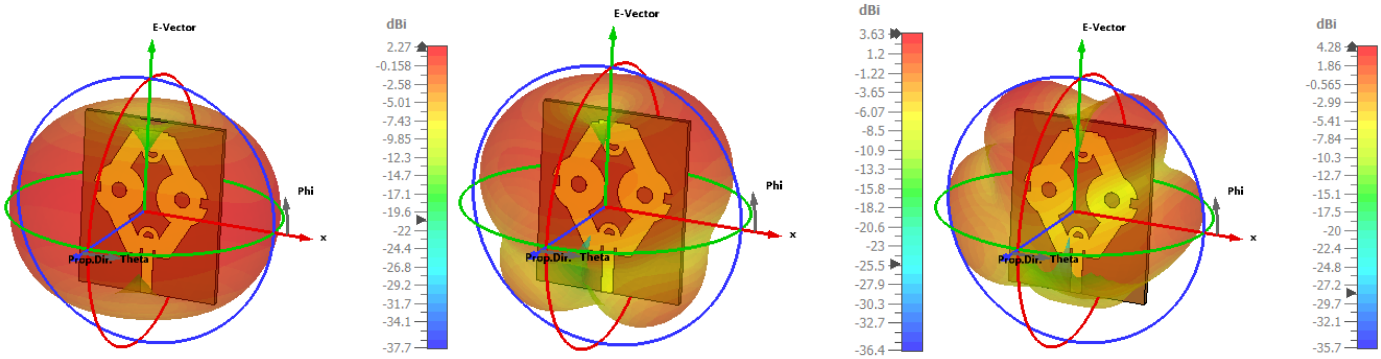

f=2.45GHz **f=4.78GHz** **f=7.6GHz**

Figure 8. Gain diagrams of the Prop-Ant at resonant frequencies obtained by simulation

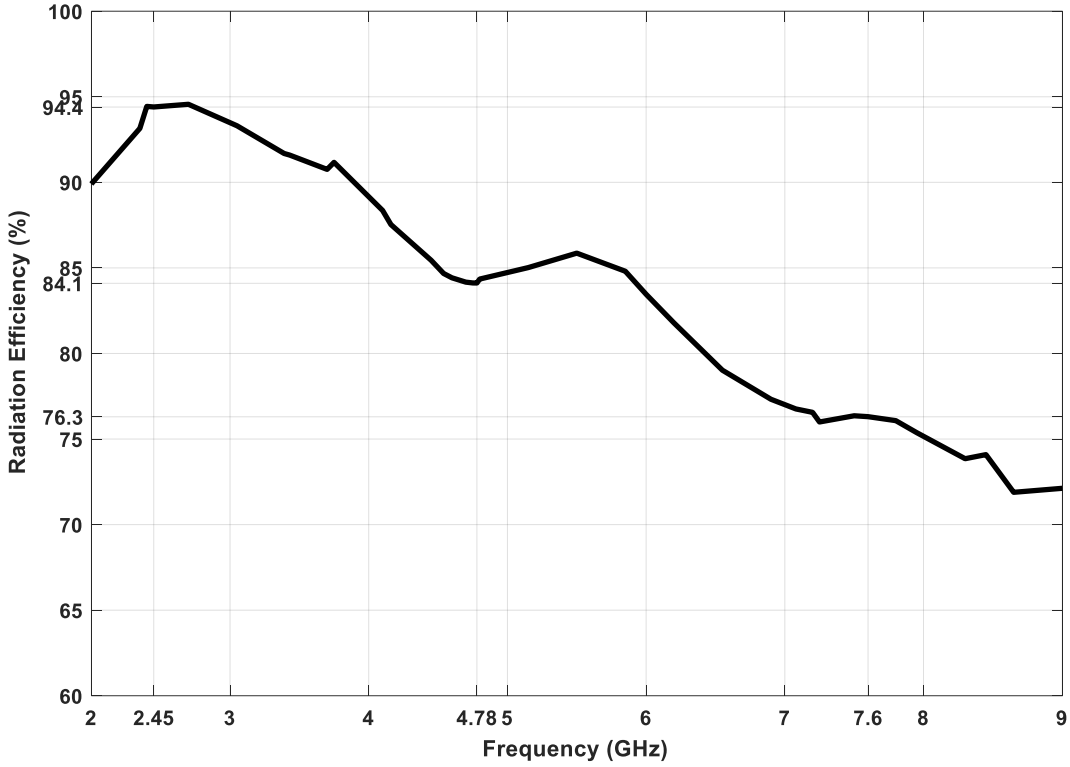

Figure 9. Simulation of the Prop-Ant's radiation efficiency

The voltage standing wave ratio (VSWR) of the Prop-Ant at resonant frequencies is shown in Figure 10. Here, the VSWRs at the resonant frequencies of 2.45GHz, 4.78GHz, and 7.6GHz are 1.09, 1.13, and 1.29, respectively. As can be seen from this figure, the VSWR is less than 2 in all three operating bands, which indicates that the impedance matching is verified in the given bands. As a result, it can be concluded that the Prop-Ant meets this requirement.

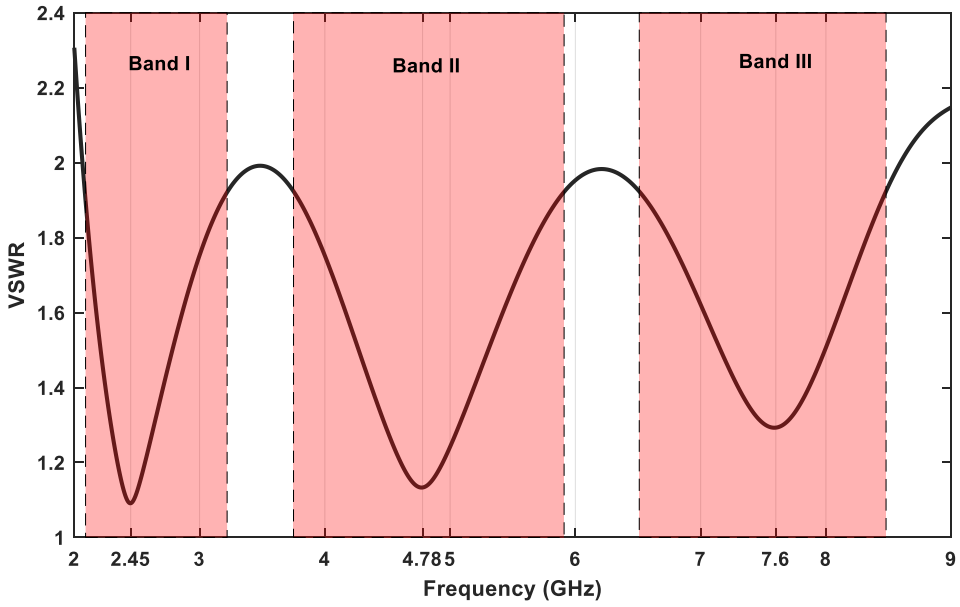

Figure 10. Variation of voltage standing wave ratio with frequency

Table 2 shows a performance comparison between the Prop-Ant and the multiband antennas in the literature (Ali et al., 2018; Brar et al., 2018; Mark et al., 2018; Singh et al., 2019; Wang et al., 2021; Yalduz & Çizmeci, 2023) in terms of size, operating frequencies, bandwidth, and gain. It is observed that the gain of the Prop-Ant is higher than the gains of the antennas presented in the literature (Ali et al., 2018; Brar et al., 2018; Singh et al., 2019). It is clearly seen that the gains of the antennas given in the literature (Mark et al., 2018; Wang et al., 2021; Yalduz & Çizmeci, 2023) are lower than the Prop-Ant in some frequency bands and close to the gain of the Prop-Ant in other frequency bands. It can be seen that the Prop-Ant design is quite advantageous in terms of size, number of operating frequency bands, impedance bandwidth, and gain compared to other reference antennas.

Table 2. Comparison of the Prop-Ant with other multiband antennas

References	Dimensions of Antenna Structures (mm^3) and Substrate material	Operating Frequency (GHz)	Bandwidth (GHz)	Number of bands	Peak Gain (dB/dBi)	Applications
(Wang et al., 2021)	36 × 39 × 1.6 FR-4	2.45/3.55/ 5.5	2.37–2.51/ 3.3–3.8/ 5.3–5.9	Three Bands	1.14–1.69/ 2.41–2.79/ 2.68–4.02 (dBi)	WLAN/WiMAX
(Ali et al., 2018)	30 × 24.8 × 1.6 FR-4	3.1/5.52/ 7.31/9.72	3.04-3.15/ 5.44-5.72/ 6.76-7.72/ 9.42-9.98	Four Bands	1.35/1/ 1.07/1.75 (dB)	WiMAX/ Satellite TV/ X-Band
(Singh et al., 2019)	35 × 30 × 1.6 FR-4	2.48/3.16	2.41-2.56/ 3.12-3.18	Double Band	1.05/1.09 (dB)	WLAN/WiMAX
(Brar et al., 2018)	50 × 35.5 × 1.6 FR-4	1.59/ 2.02/ 2.46/3.51	1.43–1.6/ 1.94–2.1/ 2.40–2.57/ 3.45–3.6	Four Bands	1.08 (dBic)/ 1.38/0.85/0.7 (dBi)	GPS/ GLONASS/ UMTS/ WLAN/WiMAX
(Yalduz & Çizmeci, 2023)	36 × 25 × 1.6 FR-4	1.936/3.43/ 5.9/7.8	1.879-0.986/ 3.100-3.87/ 4.970-6.515/ 7.260-8.60	Four Bands	-0.16-0.61/ 1.76-2.16/ 1.87-2.6/ 2.50-3.3 (dBi)	GSM/ DSRC/ WiMAX/ WLAN /X band
(Mark et al., 2018)	40 × 32 × 1.6 FR-4	1.7/2.4/ 3.1/ 4.5	1.88-1.69/ 2.52-2.34/3.59-3.07/6.26-4.17	Four Bands	1.6/2.15/ 2.75/ 3.8 (dBi)	DCS1800/ WLAN/WiMAX
This study	37.5 × 46 × 1.6 FR-4	2.45/4.78/ 7.6	2.09-3.22/ 3.75-5.91/ 6.51-8.48	Three Bands	2.27/3.63/4.28 (dBi)	RFID/WLAN/ WiMAX/C-Band

4. Conclusions

This paper presents a multiband microstrip antenna for wireless communication applications. The antenna is designed on FR-4 substrate and has dimensions of 37.5 × 46 × 1.6mm^3. The Prop-Ant is designed and analyzed using 3D-EM simulation software. The resonant frequencies of the Prop-Ant are 2.45GHz, 4.78GHz, and 7.6GHz, with bandwidths of (2.09-3.22 GHz), (3.75-5.91 GHz), and (6.51-8.48 GHz). These bandwidths cover many applications such as RFID (2.45/5.8GHz), WiMAX (2.5/5.5GHz), and WLAN (2.4/5.2/5.8GHz), and a certain bandwidth of C band. The Prop-Ant has radiation efficiencies of 94.4 %, 84.1 %, and 76.3 % at resonant frequencies and peak gains of 2.27dBi, 3.63dBi, and 4.28dBi at resonant frequencies. In this study, the parameters of the Prop-Ant, such as reflection coefficient, directivity, and gain in the operating bands, are investigated. The results show that the Prop-Ant exhibits satisfactory performances such as high gain, good efficiency, and multiband and can be used in wireless communication systems.

References

Abdalla, M. A., Hu, Z., & Muvianto, C. (2017). Analysis and design of a triple band metamaterial simplified CRLH cells loaded monopole antenna. International Journal of Microwave and Wireless Technologies, 9(4), 903–913. https://doi.org/10.1017/S1759078716000738

Ali, T., Saadh Aw, M., & Biradar, R. C. (2018). A fractal quad-band antenna loaded with L-shaped slot and metamaterial for wireless applications. International Journal of Microwave and Wireless Technologies, 10(7), 826–834. https://doi.org/10.1017/S1759078718000272

Bakariya, P. S., Dwari, S., Sarkar, M., & Mandal, M. K. (2015). Proximity-coupled microstrip antenna for bluetooth, WiMAX, and WLAN applications. IEEE Antennas and Wireless Propagation Letters, 14, 755–758. https://doi.org/10.1109/LAWP.2014.2379611

Baytore, C., Gocen, C., Palandoken, M., Kaya, A., & Zoral, E. Y. (2019). Compact metal-plate slotted WLAN-WIMAX antenna design with USB Wi-Fi adapter application. Turkish Journal of Electrical Engineering and Computer Sciences, 27(6), 4403–4417. https://doi.org/10.3906/elk-1904-122

Bekasiewicz, A., & Koziel, S. (2018). Miniaturized uniplanar triple-band slot dipole antenna with folded radiator. Microwave and Optical Technology Letters, 60(2), 386–389. https://doi.org/10.1002/MOP.30971

Benkhadda, O., Saih, M., Chaji, K., & Reha, A. (2020). Design and analysis of rectangular microstrip patch antenna using different feeding mechanisms for 2,45 ghz applications. Journal of Advanced Research in Dynamical and Control Systems, 12(4 Special Issue), 1205–1217. https://doi.org/10.5373/JARDCS/V12SP4/20201595

Brar, R. S., Saurav, K., Sarkar, D., & Srivastava, K. V. (2018). A quad-band dual-polarized monopole antenna for GNSS/UMTS/WLAN/WiMAX applications. Microwave and Optical Technology Letters, 60(3), 538–545. https://doi.org/10.1002/MOP.31008

Chen, Y. J., Liu, T. W., & Tu, W. H. (2017). CPW-Fed Penta-Band Slot Dipole Antenna Based on Comb-Like Metal Sheets. IEEE Antennas and Wireless Propagation Letters, 16, 202–205. https://doi.org/10.1109/LAWP.2016.2569606

Gao, X., Jackson, T. J., & Gardner, P. (2017). Multiband Open-Ended Resonant Antenna Based on One ECRLH Unit Cell Structure. IEEE Antennas and Wireless Propagation Letters, 16, 1273–1276. https://doi.org/10.1109/LAWP.2016.2632299

Goswami, C., Ghatak, R., & Poddar, D. R. (2018). Multi-band bisected Hilbert monopole antenna loaded with multiple subwavelength split-ring resonators. IET Microwaves, Antennas & Propagation, 12(10), 1719–1727. https://doi.org/10.1049/IET-MAP.2017.1215

He, K., Gong, S., & Gao, F. (2015). Low-profile wideband unidirectional patch antenna with improved feed structure. Electronics Letters, 51(4), 317–319. https://doi.org/10.1049/EL.2014.4309

Joshi, M. P., & Gond, V. J. (2019). Design and analysis of microstrip patch antenna for wlan and vehicular communication. Progress In Electromagnetics Research C, 97, 163–176. https://doi.org/10.2528/PIERC19090201

Karthikeyan, M., Sitharthan, R., Ali, T., & Roy, B. (2020). Compact multiband CPW fed monopole antenna with square ring and T-shaped strips. Microwave and Optical Technology Letters, 62(2), 926–932. https://doi.org/10.1002/MOP.32106

Kumar Naik, K., & Amala Vijaya Sri, P. (2018). Design of Concentric Circular Ring Patch with DGS for Dual-Band at Satellite Communication and Radar Applications. Wireless Personal Communications, 98(3), 2993–3001. https://doi.org/10.1007/S11277-017-5012-7/FIGURES/7

Kumar Sahu, N., Sharma, A., & Gangwar, R. K. (2017). Modified annular ring patch fed cylindrical dielectric resonator antenna for WLAN/WIMAX applications. Microwave and Optical Technology Letters, 59(1), 120–125. https://doi.org/10.1002/MOP.30238

Li, H., Zhou, Y., Mou, X., Ji, Z., Yu, H., & Wang, L. (2014). Miniature four-band CPW-fed antenna for RFID/WiMAX/WLAN applications. IEEE Antennas and Wireless Propagation Letters, 13, 1684–1688. https://doi.org/10.1109/LAWP.2014.2345564

Mahendran, K., Gayathri, D. R., & Sudarsan, H. (2021). Design of multi band triangular microstrip patch antenna with triangular split ring resonator for S band, C band and X band applications. Microprocessors and Microsystems, 80, 103400. https://doi.org/10.1016/J.MICPRO.2020.103400

Mark, R., Mishra, N., Mandal, K., Sarkar, P. P., & Das, S. (2018). Hexagonal ring fractal antenna with dumb bell shaped defected ground structure for multiband wireless applications. AEU - International Journal of Electronics and Communications, 94, 42–50. https://doi.org/10.1016/J.AEUE.2018.06.039

Radar Systems Panel. (2019). 521-2019 - IEEE Standard Letter Designations for Radar-Frequency Bands. IEEE Aerospace and Electronic Systems. https://ieeexplore.ieee.org/document/8999849

Ran, X., Yu, Z., Xie, T., Li, Y., Wang, X., & Huang, P. (2020). A novel dual-band binary branch fractal bionic antenna for mobile terminals. International Journal of Antennas and Propagation, 2020. https://doi.org/10.1155/2020/6109093

Singh, G., Kanaujia, B. K., Pandey, V. K., Gangwar, D., & Kumar, S. (2019). Design of compact dual-band patch antenna loaded with D-shaped complementary split ring resonator. Journal of Electromagnetic Waves and Applications, 33(16), 2096–2111. https://doi.org/10.1080/09205071.2019.1663274

Sri, P. A. V., & Ketavath, K. N. (2023). Analysis and design of trapezoidal shape CSRR rectangular patch antenna for wireless communications. Microwave and Optical Technology Letters, 65(6), 1787–1793. https://doi.org/10.1002/MOP.33619

Sura, P. R., Sekhar, M., & Andhe, K. K. (2022). Quad Band Printed Antenna for Wi-Fi, WLAN, C-band and WiMAX Applications. Wireless Personal Communications, 124(1), 437–448. https://doi.org/10.1007/S11277-021-09367-2/FIGURES/7

Verma, S., & Kumar, P. (2014). Compact triple-band antenna for WiMAX and WLAN applications. Electronics Letters, 50(7), 484–486. https://doi.org/10.1049/EL.2013.4313

Wang, S., Kong, F., Li, K., & Du, L. (2021). A planar triple-band monopole antenna loaded with an arc-shaped defected ground plane for WLAN/WiMAX applications. International Journal of Microwave and Wireless Technologies, 13(4), 381–389. https://doi.org/10.1017/S1759078720001099

Yalduz, H., & Çizmeci, H. (2023). Design and analysis of multi-band compact microstrip antenna in gsm1900/wlan/wimax/dsrc/x-band frequency bands for vehicle applications. Journal of scientific reports-a, 052, 407–418. Https://doi.org/10.59313/jsr-a.1201301